

Well-balanced finite difference weighted essentially non-oscillatory schemes for the Euler equations with static gravitational fields

Gang Li^{a,b}, Yulong Xing^{c,*}

^a School of Mathematics and Statistics, Qingdao University, Qingdao, Shandong 266071, PR China

^b Institute of Applied Mathematics from Shandong Province, Qingdao, Shandong 266071, PR China

^c Department of Mathematics, Ohio State University, Columbus, OH 43210, USA

ARTICLE INFO

Article history:

Available online 8 November 2017

Keywords:

Euler equations
Gravitational fields
WENO schemes
Well-balanced property
Hydrostatic equilibrium state
High order accuracy

ABSTRACT

Euler equations of compressible gas dynamics, coupled with a source term due to the gravitational fields, often appear in many interesting astrophysical and atmospheric applications. In this paper, we design high order finite difference weighted essentially non-oscillatory (WENO) methods for the Euler equations under static gravitational fields, which are well-balanced for known steady state solutions. We simplify the well-balanced WENO methods designed in Xing and Shu (2013) for the isothermal equilibrium, and then extend them to more general steady state solutions which include both isothermal and polytropic equilibria. One- and two-dimensional numerical examples are provided at the end to test the performance of the proposed WENO methods and verify these properties numerically.

© 2017 Elsevier Ltd. All rights reserved.

1. Introduction

In this paper, we design high order finite difference weighted essentially non-oscillatory (WENO) methods for the Euler equations under static gravitation fields, which are well-balanced for known steady state solutions. The mathematical model under consideration is the Euler equations of compressible gas dynamics, coupled with a source term due to the gravitational fields. This is an important model appearing in many interesting astrophysical and atmospheric applications. It takes the form of

$$\begin{aligned} \rho_t + \nabla \cdot (\rho \mathbf{u}) &= 0, \\ (\rho \mathbf{u})_t + \nabla \cdot (\rho \mathbf{u} \otimes \mathbf{u} + p \mathbf{I}_d) &= -\rho \nabla \phi, \\ E_t + \nabla \cdot ((E + p) \mathbf{u}) &= -\rho \mathbf{u} \cdot \nabla \phi, \end{aligned} \quad (1)$$

where $\mathbf{x} \in \mathbb{R}^d$ ($d = 1, 2, 3$) is the spatial variable, and t is the time. Here ρ , \mathbf{u} , p stand for the fluid density, the velocity, and the pressure, respectively. In this paper, $\phi = \phi(\mathbf{x})$ denotes the time independent gravitational potential, and we leave the case of time dependent ϕ for future research. \mathbf{I}_d is the identity matrix, and the operators ∇ , $\nabla \cdot$ and \otimes are the gradient, divergence and tensor product in \mathbb{R}^d , respectively. $E = \rho \|\mathbf{u}\|^2/2 + \rho e$ (with e being the internal energy) is the non-gravitational energy. To close the system, the pressure p is linked to ρ and e through the so called equation of state, denoted by $p = p(\rho, e)$. The ideal gas law, given by

$$p = (\gamma - 1)\rho e = (\gamma - 1)(E - \rho \|\mathbf{u}\|^2/2), \quad (2)$$

* Corresponding author.

E-mail addresses: gangli1978@163.com (G. Li), xing.205@osu.edu (Y. Xing).

where γ is the ratio of specific heats, is used in the numerical tests, but we would like to mention that the methods presented in this paper are applicable beyond the ideal gas equation of state.

Many existing numerical methods, including finite difference, finite volume and finite element discontinuous Galerkin (DG) methods, have been designed for the Euler equations without the source term due to gravitational fields. However, new numerical challenge emerges with the addition of the gravitational source term, as such model now admits non-trivial steady state solutions with two well-known hydrostatic steady states being the isothermal and the polytropic equilibria. Many practical applications involve the nearly steady state solutions, which are often small perturbations of these steady states. Standard numerical methods fail to balance the numerical approximations of the flux term and the source term at steady state, and introduce error comparable with the size of the physical interesting perturbation, which leads to non-physical oscillating solutions. Well-balanced methods, which can preserve the steady state solution exactly in the discrete level, are introduced to provide an efficient way to capture these small perturbations on relatively coarse meshes. Well-balanced methods for the Euler equations with gravitation were first considered by LeVeque and Bale [1], where they extended their quasi-steady wave propagation methods designed for the shallow water equations to the Euler equations. After this pioneer work, many well-balanced methods [2–8] have been designed and studied. Among them, we designed high order well-balanced finite difference WENO methods for the isothermal equilibrium in [9]. Other high order well-balanced methods can be found in [10–13], which include finite difference, finite volume and finite element DG methods.

In this paper, we propose to extend the well-balanced finite difference WENO methods designed by us in [9] for the isothermal equilibrium to more general steady state solutions which include both isothermal and polytropic equilibria. The main idea to achieve the well-balanced property is to rewrite the source terms in a special way using the information of the equilibrium state to be preserved and then discretize them using a WENO differential operator which is consistent to that for the flux term. This technique has been applied in [14–16] for the shallow water equations, and later generalized for various models including the pollutant transport equations, chemosensitive movement equation, nozzle flow, Euler equations with gravitation, and chemical reaction problems, etc. The major contribution of this paper is to first simplify the source term evaluation of the well-balanced methods in [9] which will lead to a reduced computational cost, and then extend this technique to the polytropic and other general steady state solution of the Euler equations under gravitation.

This paper is organized as follows. In Section 2, we start with presenting the mathematical model and the corresponding steady state solutions, and then propose a novel one-dimensional high order well-balanced WENO scheme, which can conserve the equilibrium state solutions exactly, and at the same time is genuinely high order accurate for the general solutions. We then extend the proposed well-balanced method to multi-dimensional problems in Section 3. Section 4 contains extensive one- and two-dimensional numerical results to demonstrate the behavior of the proposed methods, such as high order accuracy, the well-balanced property, and good resolution for smooth and discontinuous solutions. Conclusion remarks are given in Section 5.

2. Well-balanced WENO schemes for one-dimensional problems

In this section, we present our high order well-balanced finite difference WENO schemes for the Euler equations with gravitation. The simpler one-dimensional problem is discussed in this section to illustrate the main idea, and their generalization to multi-dimensional case will be given in Section 3.

2.1. Mathematical model and steady states

In one spatial dimension, the Euler equations under gravitation (1) become

$$\begin{aligned}\rho_t + (\rho u)_x &= 0, \\ (\rho u)_t + (\rho u^2 + p)_x &= -\rho \phi_x, \\ E_t + ((E + p)u)_x &= -\rho u \phi_x,\end{aligned}\quad (3)$$

where u is the one-dimensional velocity. The hydrostatic equilibrium state with a zero velocity is given by

$$u = 0, \quad p_x = -\rho \phi_x, \quad (4)$$

where the source term due to the gravitational forces is balanced by the pressure gradient. Two important special equilibria, which correspond to constant temperature (isothermal equilibrium) and constant entropy (polytropic equilibrium), are commonly encountered in the practical applications.

The isothermal equilibrium state with the constant temperature T_0 is given by

$$\rho = \rho_0 \exp\left(-\frac{\phi}{RT_0}\right), \quad u = 0, \quad p = p_0 \exp\left(-\frac{\phi}{RT_0}\right), \quad (5)$$

where $p_0 = \rho_0 RT_0$ and R is the gas constant. The polytropic hydrostatic equilibrium usually takes the form of

$$p = K \rho^\gamma. \quad (6)$$

Combined with the steady state solution (4), this will lead to the explicit form of

$$\rho = \left(\frac{\gamma - 1}{K\gamma} (C - \phi) \right)^{\frac{1}{\gamma-1}}, \quad u = 0, \quad p = \frac{1}{K^{\frac{1}{\gamma-1}}} \left(\frac{\gamma - 1}{\gamma} (C - \phi) \right)^{\frac{\gamma}{\gamma-1}}, \tag{7}$$

where C and K are both constants. As shown in [5], the polytropic equilibrium (7) can also be written as

$$u = 0, \quad h + \phi = C, \tag{8}$$

where $h = e + p/\rho$ denotes the specific enthalpy. Because of the nonlinear relationship between ρ and p of the polytropic equilibrium, it is usually more challenging to design well-balanced methods for such steady state.

2.2. Review of finite difference WENO methods

For the sake of simplicity, we assume that the grid points $\{x_j\}$ are uniformly distributed with step size $\Delta x = x_{j+1} - x_j$. We take the one-dimensional scalar hyperbolic conservation laws

$$v_t + f(v)_x = 0, \tag{9}$$

as an example to present a quick review of the finite difference WENO scheme. The complete algorithm can be found in [17] and the recent review paper by Shu in [18]. The computational variables of the semi-discrete WENO methods are denoted by $v_j(t)$, which approximate the point values $v(x_j, t)$. The WENO scheme takes the form of

$$\frac{dv_j(t)}{dt} + \frac{1}{\Delta x} (\widehat{f}_{j+\frac{1}{2}} - \widehat{f}_{j-\frac{1}{2}}) = 0, \tag{10}$$

with $\widehat{f}_{j+\frac{1}{2}}$ being the numerical fluxes to be defined below, which approximate $h_{j+\frac{1}{2}} = h(x_{j+\frac{1}{2}})$ with high order accuracy. Herein, $h(x)$ is implicitly defined by

$$f(v(x)) = \frac{1}{\Delta x} \int_{x-\Delta x/2}^{x+\Delta x/2} h(\xi) d\xi,$$

and we refer to [17] for the details of this function.

To ensure the numerical stability, we take the upwind idea into account and split the flux $f(v)$ into two parts

$$f(v) = f^+(v) + f^-(v),$$

where $\frac{df^+(v)}{dv} \geq 0$ and $\frac{df^-(v)}{dv} \leq 0$. One example is the simple Lax–Friedrichs flux

$$f^\pm(v) = \frac{1}{2}(f(v) \pm \alpha v), \tag{11}$$

with $\alpha = \max_v |f'(v)|$, and the maximum is taken over the whole region. Next, the WENO reconstruction idea [17] is used to obtain the numerical fluxes $\widehat{f}_{j+\frac{1}{2}}^+$ and $\widehat{f}_{j+\frac{1}{2}}^-$. For example, $\widehat{f}_{j+\frac{1}{2}}^+$ can be expressed as

$$\widehat{f}_{j+\frac{1}{2}}^+ = \sum_{k=0}^r \omega_k q_k^r (f_{j+k-r}^+, \dots, f_{j+k}^+), \tag{12}$$

where $f_i^+ = f^+(v_i)$, $i = j - r, \dots, j + r$ and

$$q_k^r(\mathbf{g}_0, \dots, \mathbf{g}_r) = \sum_{l=0}^r a_{k,l}^r g_l \tag{13}$$

provides a $(r + 1)$ th order approximation of the numerical flux on the k th stencil $S_k = (x_{j+k-r}, \dots, x_{j+k})$, $k = 0, 1, \dots, r$, with $a_{k,l}^r$, $0 \leq k, l \leq r$ being the corresponding constant coefficients (see [19] for more details). Here ω_k in (12) is the nonlinear weight which satisfies $\sum_{k=0}^r \omega_k = 1$ and is formulated as

$$\omega_k = \frac{\alpha_k}{\sum_{l=0}^r \alpha_l}, \quad \text{with } \alpha_k = \frac{C_k^r}{(\varepsilon_{\text{WENO}} + IS_k)^2}, \quad k = 0, 1, \dots, r, \tag{14}$$

where C_k^r is the linear weight to provide $(2r + 1)$ th-order accuracy in the smooth regions, and $\varepsilon_{\text{WENO}}$ is a small positive constant used to avoid the denominator becoming zero. In this paper, $\varepsilon_{\text{WENO}} = 10^{-6}$ is used for all test cases. IS_k are the smoothness indicators of $f^+(v)$ on the stencil S_k , $k = 0, 1, \dots, r$ proposed in [17,19]. The WENO reconstruction procedure

for $\widehat{f}_{j+\frac{1}{2}}^-$ can be obtained by a mirror symmetry to that for $\widehat{f}_{j+\frac{1}{2}}^+$ with respect to $x_{j+\frac{1}{2}}$. Consequently, we define the numerical flux $\widehat{f}_{j+\frac{1}{2}}$ as follows:

$$\widehat{f}_{j+\frac{1}{2}} = \widehat{f}_{j+\frac{1}{2}}^+ + \widehat{f}_{j+\frac{1}{2}}^-,$$

which completes semi-discrete scheme (10).

Runge–Kutta methods can be used as the temporal discretization of (10) to derive fully discrete methods. In this paper, we apply the following third order Runge–Kutta method:

$$\begin{aligned} v^{(1)} &= v^n + \Delta t \mathcal{F}(v^n) \\ v^{(2)} &= \frac{3}{4}v^n + \frac{1}{4}(v^{(1)} + \Delta t \mathcal{F}(v^{(1)})) \\ v^{n+1} &= \frac{1}{3}v^n + \frac{2}{3}(v^{(2)} + \Delta t \mathcal{F}(v^{(2)})), \end{aligned} \tag{15}$$

with $\mathcal{F}(v)$ denoting the spatial operator.

2.3. Well-balanced WENO schemes

In the subsection, we present well-balanced finite difference WENO schemes to one-dimensional Euler equations with known equilibrium state (4), and also explain how they can be applied to the special cases of isothermal equilibrium (5) and polytropic equilibrium (7). In the case of isothermal equilibrium, they reduce to a simpler version of the finite difference WENO methods presented in [9], therefore this paper can also be viewed as a simplification and generalization of that well-balanced technique to more general steady states.

The general steady state solutions are given by (4), and we would like to design numerical methods which preserve such steady states which satisfy the following assumption:

The targeting steady state solutions to be preserved in (4) are explicitly known and can be denoted by $\rho^e(x)$ and $p^e(x)$ (or $\rho^e(x)$ and $E^e(x)$). (16)

Therefore, (4) leads to the fact

$$p^e(x)_x = -\rho^e(x)\phi_x. \tag{17}$$

In order to design well-balanced methods, we follow the idea in [9] to reformulate the source term using (17) and rewrite the governing equations (3) as

$$\begin{aligned} \rho_t + (\rho u)_x &= 0 \\ (\rho u)_t + (\rho u^2 + p)_x &= \frac{\rho}{\rho^e} p_x^e \\ E_t + ((E + p)u)_x &= -\rho u \phi_x, \end{aligned} \tag{18}$$

where we replace the source term $-\rho\phi_x$ in the second equation by $\frac{\rho}{\rho^e}p_x^e$. The source term in the third equation is kept the same, as it reduces to zero at the steady state (4) and therefore will not affect the well-balanced property. Let us denote this system in a compact vector form for the ease of presentation

$$U_t + F(U)_x = S,$$

where $U = (\rho, \rho u, E)^T$, $F(U)$ and S stand for the unknown vector, the flux and the source term, respectively.

The semi-discrete well-balanced WENO schemes still take the form of

$$\frac{d}{dt}U_j(t) + \frac{1}{\Delta x_j}(\widehat{F}_{j+\frac{1}{2}} - \widehat{F}_{j-\frac{1}{2}}) = S_j, \tag{19}$$

but with slightly modified numerical fluxes and source term approximations outlined below.

To present the basic idea of the modification, we first consider the situation when the WENO scheme is applied without the flux splitting (e.g., WENO-Roe scheme) or the local characteristic decomposition for the system of equations. Let us compute the numerical fluxes $\widehat{f}_{j+\frac{1}{2}}$ as stated in Section 2. As to the source term approximation, the third term $(-\rho u \phi_x)_j$ can be computed as usual, namely if ϕ_x is available, $(\phi_x)_j$ can be evaluated at the point x_j . And if ϕ is only available pointwise and there is no explicit formulation of ϕ_x , one option is to use the WENO reconstruction to compute $(\phi_x)_j$ from the point values $\phi_{j\pm k}$. At the end, we let

$$(-\rho u \phi_x)_j = -(\rho u)_j(\phi_x)_j. \tag{20}$$

For the second source term $\frac{\rho}{\rho^e} p_x^e$, we use the usual WENO reconstruction to compute $\widehat{p}_{j+1/2}^e$ from the point values $p_{j\pm k}^e$, and then approximate $(p_x^e)_j$ by $(\widehat{p}_{j+1/2}^e - \widehat{p}_{j-1/2}^e) / \Delta x_j$ to obtain

$$\left(\frac{\rho}{\rho^e} p_x^e\right)_j = \frac{\rho_j}{\rho_j^e} \frac{\widehat{p}_{j+1/2}^e - \widehat{p}_{j-1/2}^e}{\Delta x_j}. \tag{21}$$

With the standard WENO numerical flux and source term approximation stated above, this WENO method without any further modification is actually well-balanced, and we refer to [Proposition 1](#) for the detailed proof.

Next, we look at the situation when the WENO procedure involves the local characteristic decomposition, which is often used for the system of equations including the Euler equations. The local characteristic matrix R , consisting of the right eigenvectors of the Jacobian at $v_{j+1/2}$, is used to compute the numerical flux at $x_{j+1/2}$. All the neighboring point values of the vectors $(\rho u, \rho u^2 + p, (E + p)u)_{j\pm k}$ are projected to the local characteristic fields determined by R^{-1} , and the WENO reconstruction is then completed in the characteristic space. After the WENO reconstruction, the value will be projected back to the physical space to obtain $\widehat{F}_{j+1/2}$. For the source term approximation, we mimic the process and project the vector $(0, p^e(x), 0)_{j\pm k}$ to the local characteristic fields to carry out the WENO reconstruction. The reconstructed value is projected back to obtain $\widehat{p}_{j+1/2}^e$ for the source term approximation.

Finally, we consider WENO schemes with a Lax–Friedrichs flux splitting, denoted by the WENO-LF scheme. The flux $F(U)$ is separated into two parts:

$$F(U) = F^+(U) + F^-(U),$$

where

$$F^\pm(U) = \frac{1}{2} (F(U) \pm \alpha_i U), \tag{22}$$

with

$$\alpha_i = \max_U |\lambda_i(U)|$$

for the i th characteristic field and $\lambda_i(U)$ being the i th eigenvalue of the Jacobian $\partial F(U) / \partial U$. The $\pm \alpha_i U$ term contributes to the numerical viscosity, which is essential for the numerical approximation of hyperbolic conservation laws. But such term may destroy the well-balanced property at the steady state solution. Therefore, we propose to modify the flux splitting as follows

$$F^\pm(U) = \frac{1}{2} (F(U) \pm \alpha'_i \widetilde{U}), \tag{23}$$

with \widetilde{U} given by

$$\widetilde{U} = \left(\frac{\rho}{\rho^e}, \frac{\rho u}{\rho^e}, \frac{E}{p^e} \right),$$

and the coefficient α'_i defined as

$$\alpha'_i = \alpha_i \max_j (\rho_j^e, p_j^e).$$

At the steady state [\(4\)](#), \widetilde{U} becomes the constant, and the effect of this viscosity term $\pm \alpha'_i \widetilde{U}$ towards the approximation of $F(U)_x$ is zero. An alternative is to replace \widetilde{U} by

$$\widetilde{U} = (\rho - \rho^e, \rho u, E - p^e / (\gamma - 1)),$$

and $\alpha'_i = \alpha_i$, which will serve the same purpose. As the flux splitting WENO approximation becomes $F^\pm(U) = F(U) / 2$ at the steady state, the well-balanced source term approximation can be obtained if we simply split the derivatives in the second source term as:

$$\begin{pmatrix} 0 \\ p_x^e \\ 0 \end{pmatrix} = \begin{pmatrix} 0 \\ p_x^e / 2 \\ 0 \end{pmatrix} + \begin{pmatrix} 0 \\ p_x^e / 2 \\ 0 \end{pmatrix}, \tag{24}$$

and apply the same WENO procedure corresponding to F^+ or F^- to approximate them respectively. We then add up the resulting $\widehat{p}_{j+1/2}^{\pm}$ to obtain

$$\widehat{p}_{j+1/2}^e = \widehat{p}_{j+1/2}^{e+} + \widehat{p}_{j+1/2}^{e-}. \tag{25}$$

For the numerical methods described above, we have

Proposition 1. For the Euler equations with gravitation [\(3\)](#), reformulated in the form of [\(18\)](#), the semi-discrete finite difference WENO schemes [\(19\)](#), with the standard WENO numerical fluxes for WENO-Roe or modified numerical fluxes based on [\(23\)](#)

for WENO-LF, combined with the source term approximation stated in (20)–(21) for WENO-Roe or modified source term approximation with (20), (21), (24), (25) for WENO-LF, are well-balanced for the general steady state solution (4) satisfying the assumption (16).

Proof. We use the WENO-Roe method as an example to prove the well-balanced property. The proof of WENO-LF method follows the same way and is ignored here to save space. At the steady state (4) where $u = 0$ and $p = p^e(x)$, the flux $F(U)$ becomes

$$F(U) = \begin{pmatrix} \rho u \\ \rho u^2 + p \\ (E + p)u \end{pmatrix} = \begin{pmatrix} 0 \\ p^e \\ 0 \end{pmatrix},$$

and the numerical flux $\hat{F}_{j+1/2}$ are obtained by the standard WENO reconstruction on $F(U)$. The third source term approximation $(-\rho u \phi_x)_j$ becomes 0 since $u = 0$, and the second source term approximation reduced to $(\frac{\rho}{\rho^e} p_x^e)_j = (p_x^e)_j$ which is computed by the WENO reconstruction. Therefore, the flux and source term approximation reduce to the same WENO reconstruction for $(p^e)_x$, and cancel with each other, which leads to the desired well-balanced property. □

We now summarize the complete procedure of the high order well-balanced finite difference WENO-LF scheme for solving the one-dimensional Euler equations (3):

1. Reformulate the source term and rewrite the equation in the form (18).
2. Approximate the derivative term in the source term of momentum equation in (18) by splitting them as in (24) and then applying the standard WENO procedure with flux splitting on them to obtain $\hat{p}_{j+1/2}^e$ as in (25). Approximate the derivative term in the source term of energy equation in a straightforward way.
3. At each time step, perform the usual WENO-LF approximation on the flux derivative $F(U)_x$ with a modified flux splitting (23).
4. Evaluate the source term at the current time step by (20) and (21) using the derivative term approximation from Step 2.
5. Add up the residues of the numerical flux and source term approximations, and forward in time by Runge–Kutta methods.

2.3.1. Isothermal equilibrium

Now, let us consider the special case of the isothermal equilibrium given by (5). Therefore, we have $\rho^e(x) = \rho_0 \exp\left(-\frac{\phi}{RT_0}\right)$ and $p^e(x) = p_0 \exp\left(-\frac{\phi}{RT_0}\right)$. As explained above, the required steps to obtain well-balanced finite difference WENO methods include: (1) rewriting the source term of the momentum equation as $-\rho g = \frac{\rho}{\rho^e} p_x^e$; (2) evaluating this source term numerically via (21); and (3) modifying the numerical flux by (23). As proven in Proposition 1, the finite difference WENO methods after these modifications satisfy the well-balanced property.

Remark 1. Finite difference well-balanced WENO numerical methods for the Euler equations under gravity have been proposed in [9]. The method proposed there is very similar to the one described above, with the only difference in the source term evaluation (21). In [9], $\hat{p}_{j+1/2}^e$ are computed by applying the WENO reconstruction procedure on p_j^e with the weights computed from the WENO reconstruction of the flux F_j . In this paper, we simplify the procedure by applying the WENO reconstruction on p_j^e directly (with the weights computed from p_j^e). The difference in these two approximations also leads to the following difference in the implementation. In [9], $\hat{p}_{j+1/2}^e$, hence the source term approximation, needs to be re-evaluated at each time step as the weights from the WENO reconstruction of the flux F_j may change at different time. If the method described in this paper is used, we can simply compute $\hat{p}_{j+1/2}^e$ once at the beginning of the code and use them for all the time steps, hence save some computational costs, for solving the Euler equations with static gravitational fields. The approach in this paper can be viewed as a simplification and generalization of the well-balanced methods studied in [9].

2.3.2. Polytropic equilibrium

Next, we turn our attention to the polytropic equilibrium given by (7). Therefore, we have $\rho^e(x) = \left(\frac{\gamma-1}{K\gamma}(C - \phi)\right)^{\frac{1}{\gamma-1}}$ and $p^e(x) = \frac{1}{K^{\frac{1}{\gamma-1}}} \left(\frac{\gamma-1}{\gamma}(C - \phi)\right)^{\frac{\gamma}{\gamma-1}}$. The same three steps listed in Section 2.3.1 can be applied to generate well-balanced finite difference WENO methods.

3. Multi-dimensional extension

The approach to design one-dimensional finite difference well-balanced WENO methods can be easily extended to multi space dimensions, which will be explained in this section. Consider the multi-dimensional Euler equations (1) under the

gravitation, the isothermal equilibrium takes the form of

$$\rho = \rho_0 \exp\left(-\frac{\phi}{RT_0}\right), \quad \mathbf{u} = \mathbf{0}, \quad p = RT\rho = RT\rho_0 \exp\left(-\frac{\phi}{RT_0}\right), \quad (26)$$

and the polytropic equilibrium is given by

$$\rho = \left(\frac{\nu - 1}{K\nu}(C - \phi)\right)^{\frac{1}{\nu-1}}, \quad \mathbf{u} = \mathbf{0}, \quad p = \frac{1}{K^{\frac{1}{\nu-1}}}\left(\frac{\nu - 1}{\nu}(C - \phi)\right)^{\frac{\nu}{\nu-1}}. \quad (27)$$

Extension of standard finite difference WENO schemes to multi space dimensions on rectangular meshes is straightforward, and can be obtained dimension by dimension directly. Let us take two dimension as an example. For every fixed j , we can define $G(x) = F(U(x, y_j))$, and then apply the one-dimensional WENO reconstruction to approximate $G'(x_i) = F_x(U(x_i, y_j))$. We can repeat it to approximate $F_y(U(x_i, y_j))$ by fixing i and defining $H(y) = F(U(x_i, y))$. We refer to [17,19] for more details of multi-dimensional finite difference WENO methods.

Following the steps to design well-balanced WENO methods for the one-dimensional problem, we first define the equilibrium state $\rho^e(\mathbf{x})$, $p^e(\mathbf{x})$ (for example the density and pressure in Eqs. (26) or (27)), and then rewrite the source term in the momentum equation of (1) as

$$-\rho \nabla \phi = \frac{\rho}{\rho^e} \nabla p^e.$$

The one-dimensional well-balanced procedure to approximate the derivatives of the flux term and source term, described in Section 2.3, will be applied in each of the \mathbf{x} directions. As summarized in Section 2.3.1, in addition to the standard WENO-LF procedure, we need to modify the viscosity part of the flux splitting in the numerical flux evaluation as in (23) and approximate the derivative ∇p^e in the source term by the splitting (24) and the standard WENO reconstruction. For the temporal discretization, TVD Runge–Kutta method (15) can be used.

Easy to verify that, all the desired properties proved in the one-dimensional case, such as high order accuracy, and well-balanced property, are still valid in the multi-dimensional case.

4. Numerical results

In this section, we demonstrate the performance of the proposed WENO schemes by extensive one- and two-dimensional numerical results. The fifth order finite difference WENO schemes, coupled with third order TVD Runge–Kutta time discretization methods (15), are used in all the tests. The CFL number is taken as 0.6. Since the paper [9] contains a series of numerical results to test the performance of well-balanced finite difference WENO methods for the isothermal equilibrium state, here we only include the well-balanced tests for the polytropic equilibrium (7) or (27) to save space.

4.1. Accuracy test

In the first example, we test the order of accuracy of the proposed well-balanced WENO schemes, and consider the following initial data [7]

$$\begin{aligned} \rho(x, 0) &= \exp(-x), \\ u(x, 0) &= 0, \\ p(x, 0) &= (1 + x) \exp(-x), \end{aligned}$$

coupled with the gravitational potential $\phi(x) = x^2/2$ and $\gamma = 1.4$ in a unit computational domain $[0, 1]$. The time step Δt is taken to be proportional to $\Delta x^{5/3}$, so that the temporal accuracy matches the spatial accuracy. We run this example up to the final time of $t = 0.1$. As the exact solution is not available, we apply the same method with a much refined mesh of 6400 points to obtain a reference solution numerically. Table 1 shows the numerical errors in L^1 norm and the order of accuracy. We can see that finite difference WENO methods converge with the expected fifth order accuracy. The L^∞ and L^2 errors demonstrate a similar pattern as the L^1 errors, therefore we only list the L^1 errors in the paper to save the space.

4.2. Hydrostatic atmosphere in a linear gravitational field

In this example, we consider a polytropic hydrostatic atmosphere, studied in [5,11]. The gravitation field is given by $\phi(x) = gx$ with $g = 1$, and the polytropic equilibrium state takes the form of

$$\begin{aligned} \rho(x) &= \left(\rho_0^{\gamma-1} - \frac{1}{K_0} \frac{\gamma-1}{\gamma} gx\right)^{\frac{1}{\gamma-1}}, \\ u(x) &= 0, \\ p(x) &= K_0 \rho(x)^\gamma, \end{aligned} \quad (28)$$

with $\gamma = 5/3$, $\rho_0 = 1$, $p_0 = 1$ and $K_0 = p_0/\rho_0^\gamma$ in a computational domain $[0, 2]$.

Table 1
 L^1 errors and numerical orders of accuracy for the test case in Section 4.1.

N	ρ		ρu		E	
	L^1 error	Order	L^1 error	Order	L^1 error	Order
25	1.17E-2		3.71E-2		1.89E-2	
50	1.45E-3	3.01	4.64E-3	3.00	2.57E-3	2.88
100	1.16E-4	3.65	3.57E-4	3.70	2.00E-4	3.69
200	5.57E-6	4.38	1.70E-5	4.39	8.72E-6	4.52
400	2.00E-7	4.80	6.50E-7	4.71	3.07E-7	4.83
800	6.29E-9	4.99	1.99E-8	5.03	9.27E-9	5.05

Table 2
 L^1 errors for different precisions for the steady state solution in Section 4.2.1.

N	Precision	ρ	ρu	E
100	Single	5.36E-08	2.99E-08	5.02E-08
	Double	4.99E-15	6.17E-16	2.43E-16
200	Single	7.60E-08	3.25E-08	5.94E-08
	Double	1.03E-14	1.23E-15	5.03E-16

4.2.1. Well-balanced property

We take the polytropic equilibrium (28) as the initial condition, and use it to test the well-balanced property of the proposed finite difference WENO methods. The example is run to the final time $t = 4$ with both 100 and 200 points. To demonstrate that the numerical error is maintained at the round-off level, we carry out the simulation with both single precision and double precision. The L^1 errors of numerical solutions with various spatial points and precisions are shown in Table 2, where we can observe that the equilibrium states are maintained up to the round-off level. This verifies the desired well-balanced property.

4.2.2. Small amplitude wave propagation

In the second test case, we would like to compare the ability of capturing small amplitude perturbation between the well-balanced WENO schemes and non-well-balanced ones. So we impose a periodic velocity perturbation

$$u(x, t) = A \sin(4\pi t), \tag{29}$$

at the bottom of the atmosphere, with $A = 10^{-6}$ representing a small perturbation. The excited waves move through the computational domain and are modified by the density and pressure stratification of the atmosphere. We run the simulation until $t = 1.5$ with 200 points. Again, we use the same fifth order well-balanced WENO scheme with a much refined 2000 points to compute a reference solution. To demonstrate the advantage of well-balanced methods, we also run the same test with non-well-balanced WENO schemes on 200 points using the straightforward source term evaluation. The pressure perturbations and the velocity of both methods at the final time, as well as those of the reference solution, are shown in Fig. 1. Easy to observe that the solution of well-balanced WENO schemes is in good agreement with the reference solution, which demonstrates that the importance of the well-balanced methods in capturing small amplitude perturbations to the steady state.

4.2.3. Large amplitude wave propagation

In this test case, we repeat the simulation, but with a large amplitude perturbation $A = 0.1$ in (29). The numerical results at time $t = 1.5$ are displayed in Fig. 2. We observe that both well-balanced and non-well-balanced schemes produce satisfying results, which agrees with our expectation that the well-balanced methods perform similarly as non-well-balanced methods when far away from the steady states.

4.3. Contact discontinuity under gravitational field

Here we consider a Riemann problem under the gravitational field $\phi_x = 1$ acting in the negative x direction. Following the setup in [7, 11], the initial conditions consist of a jump at $x = 0.5$ and are given by

$$(\rho, u, p) = \begin{cases} (1, 0, 1) & \text{if } x \leq 0.5, \\ (10, 0, 1) & \text{otherwise,} \end{cases}$$

with $\gamma = 1.4$ in a unit computational domain $[0, 1]$. The solid wall boundary condition is imposed on both end points.

We compute this problem to the stopping time of $t = 0.6$, and plot the numerical solutions obtained with 200 points in Fig. 3. For comparison, we use the same fifth order WENO scheme with a much refined $N = 2000$ points to compute a reference solution, and include them in the plots. By comparing the results, we can easily observe that the discontinuities are well solved by the proposed methods even on the relatively coarse mesh, and the numerical solutions agree well with the reference ones. In addition, we also include the numerical results of the non-well-balanced WENO schemes in the figures, and observe a better performance of the well-balanced methods over the non-well-balanced ones.

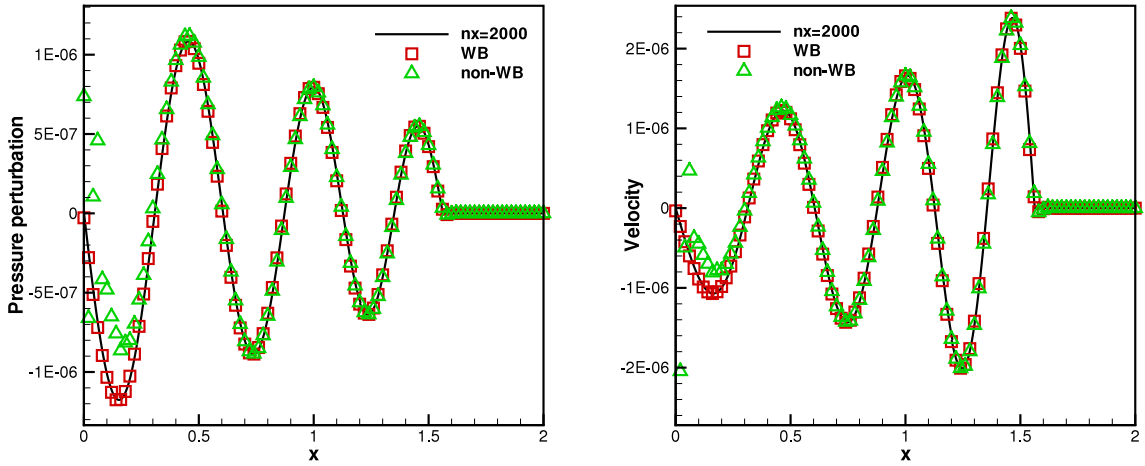


Fig. 1. Small amplitude waves traveling up the hydrostatic atmosphere in Section 4.2.2: the pressure perturbations (left) and velocity (right). Included are the solution of well-balanced (denoted by WB) schemes with 200 and 2000 points, and that of the non-well-balanced (denoted by non-WB) schemes with 200 points.

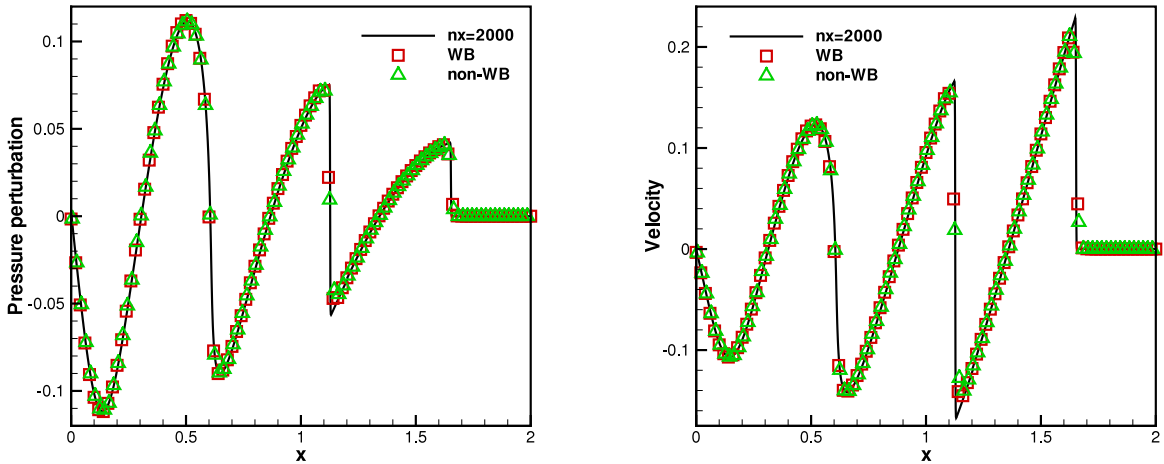


Fig. 2. Large amplitude waves traveling up the hydrostatic atmosphere in Section 4.2.3: the pressure perturbations (left) and velocity (right). Included are the solution of well-balanced schemes with 200 and 2000 points, and that of the non-well-balanced schemes with 200 points.

4.4. Two-dimensional polytrope

Subsequently, we consider two-dimensional test cases to test the performance of the proposed methods. In this example taken from [5,12], we consider a static adiabatic gaseous sphere holding together by self-gravitation. From the hydrostatic equilibrium

$$\frac{dp}{dr} = -\rho \frac{d\phi}{dr}, \tag{30}$$

and the Poisson equation for the gravitational field $\phi(r)$, one can derive an analytical solution for $\gamma = 2$ (neutron stars can be modeled by $\gamma = 2-3$). The density, pressure and velocity of the analytical equilibrium are given as follows

$$\rho^e(x, y) = \rho^e(r) = \rho_c \frac{\sin(\alpha r)}{\alpha r}, \quad p^e(x, y) = p^e(r) = K\rho(r)^2, \quad \mathbf{u}^e = 0, \tag{31}$$

and the gravitational potential is given by

$$\phi(x, y) = \phi(r) = -2K\rho_c \frac{\sin(\alpha r)}{\alpha r}, \tag{32}$$

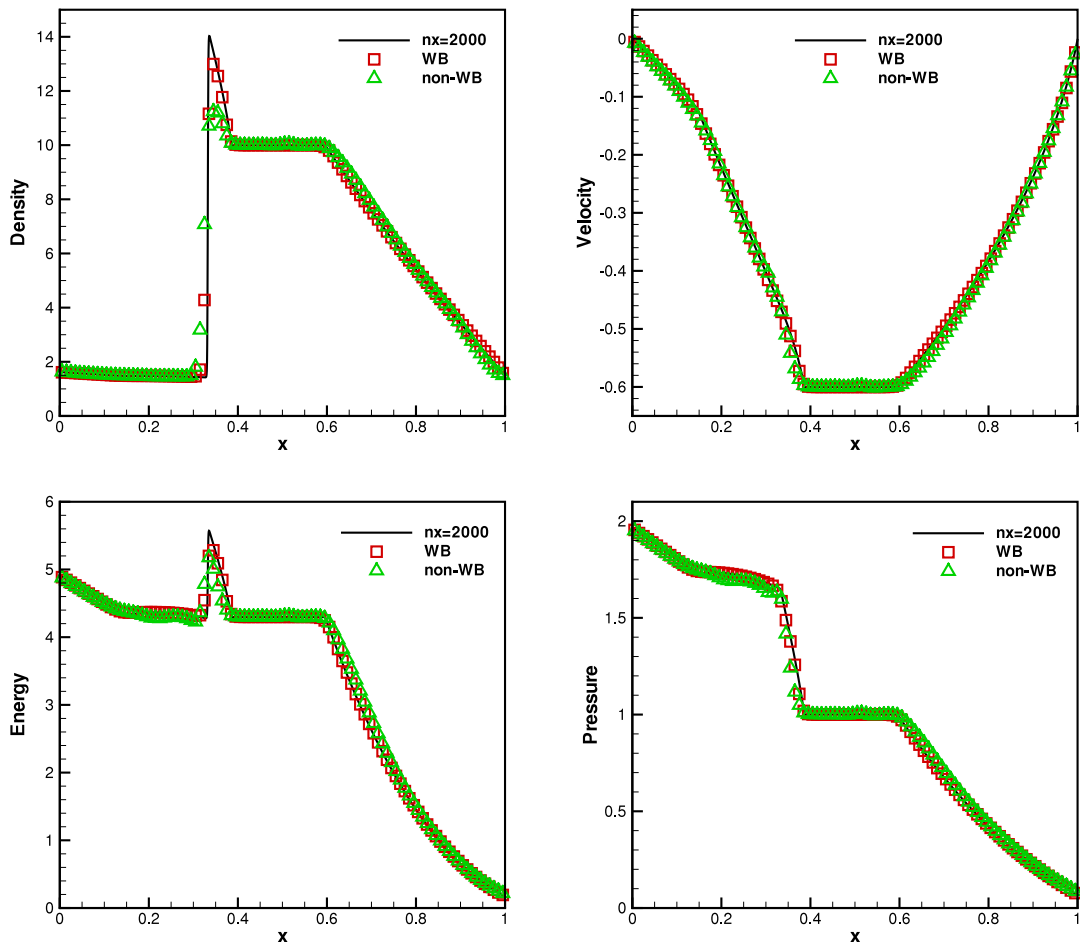


Fig. 3. Contact discontinuity under gravitational field in Section 4.3. Included are the solution of well-balanced schemes with 200 and 2000 points, and those of the non-well-balanced scheme with 200 points. Top left: density distribution; Top right: velocity distribution; Bottom left: energy distribution; Bottom right: pressure distribution.

Table 3

L^1 errors for different precisions for the steady state solution (31) and (32) in Section 4.4.1 by well-balanced methods.

N	Precision	ρ	ρu	ρv	E
50 × 50	Single	5.89E-7	4.54E-7	4.37E-7	6.39E-7
	Double	3.96E-16	1.91E-16	1.91E-16	4.40E-15
100 × 100	Single	8.76E-6	5.70E-6	5.71E-7	6.17E-6
	Double	5.78E-15	1.99E-15	1.99E-15	9.15E-15

with $\alpha = \sqrt{\frac{4\pi g}{2K}}$ and $r = \sqrt{x^2 + y^2}$ being the radial variable on a Cartesian domain $[-0.5, 0.5] \times [-0.5, 0.5]$. Herein, we take $K = g = \rho_c = 1$ in this test. We can observe that the polytrope obviously fulfills the polytropic equality $h(r) + \phi(r) = 0$ for any $r > 0$.

4.4.1. Well-balanced property

Firstly, we test the well-balanced property of the proposed WENO methods on this two-dimensional problem, by using this equilibrium state (31) as the initial condition. We compute the solution up to $t = 14.8$ on the meshes of both 50×50 and 100×100 points. To demonstrate that the numerical error is maintained at the round-off level, we carry out the simulation with both single precision and double precision. The L^1 errors of numerical solutions with various spatial points and precisions are shown in Table 3, where we can observe that the equilibrium states are maintained up to the round-off level. This verifies the desired well-balanced property. For comparison, we also present the L^1 errors of the non-well-balanced methods in Table 4. It is evident that the L^1 errors of the non-well-balanced method are much larger than those by the well-balanced one, and they do not change much when different precisions are used.

Table 4
 L^1 errors for different precisions for the steady state solution (31) and (32) in Section 4.4.1 by non-well-balanced methods.

N	Precision	ρ	ρu	ρv	E
50×50	Single	0.2387	0.2638	0.2638	0.3258
	Double	0.2387	0.2638	0.2638	0.3259
100×100	Single	0.2362	0.2607	0.2607	0.3223
	Double	0.2362	0.2607	0.2606	0.3223

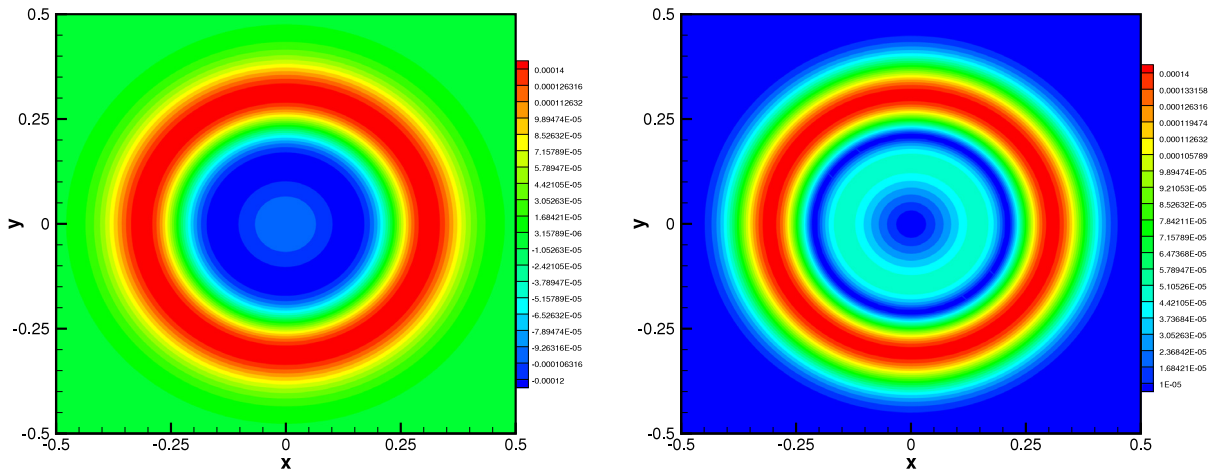


Fig. 4. The contours of the numerical results of the small amplitude wave propagation problem in Section 4.4.2 by well-balanced WENO schemes at time $t = 0.2$ with 100×100 points. Pressure perturbation (left) and velocity $(\sqrt{u^2 + v^2})$ (right).

4.4.2. Small amplitude wave propagation

In order to test the capability of the proposed method in capturing small perturbations of the hydrostatic equilibrium, we add a small Gaussian hump perturbations to the pressure profile of the equilibrium state

$$p(r) = K\rho(r)^2 + 0.001 \exp(-100r^2),$$

where $\rho(r)$ is given by as in (31), and keep the velocity and density profiles to be same. The transmission boundary conditions are applied in this test.

We evolved this modified initial condition up to $t = 0.2$ on a mesh of 100×100 uniform points and present the contour plots of the pressure perturbation and the velocity $\sqrt{u^2 + v^2}$ at the final time in Fig. 4. To demonstrate the advantage of well-balanced methods, we also run the same test with non-well-balanced WENO schemes on the same mesh using the straightforward source term evaluation, and present the results in Fig. 5. From these figures, we can observe that non-well-balanced WENO schemes are not capable of capturing such small perturbation on relatively coarse meshes, while the well-balanced ones can resolve it very well and preserve the axial symmetric structure.

Next, we compute this test case up to a longer time with both well-balanced and non-well-balanced WENO schemes. Their numerical results at $t = 1.5$ are presented in Figs. 6 and 7, respectively. Their numerical results at $t = 3$ are shown in Figs. 8 and 9, respectively. From these figures, it is obvious that the numerical solutions of non-well-balanced methods contain much larger errors when compared with those of the well-balanced methods. This phenomenon is a manifestation of that the non-well-balanced methods cannot capture the small perturbations of the hydrostatic equilibrium well on a relative coarse mesh.

4.5. Polytopic hydrostatic solution

In the last two-dimensional example, we follow the setup in [7] and consider a polytropic hydrostatic solution of the form

$$\rho^e(x, y) = (T^e(x, y))^{\frac{1}{\gamma-1}}, \quad u^e(x, y) = v^e(x, y) = 0, \quad p^e(x, y) = (T^e(x, y))^{\frac{\gamma}{\gamma-1}}, \tag{33}$$

on a unit computational domain with $T^e(x, y) = 1 - \frac{\gamma-1}{\gamma}\phi(x, y)$, $\gamma = 1.4$ and $\phi(x, y) = x + y$. In this test, we impose a small perturbation to the pressure profile

$$p(x, y, 0) = p_e + \eta \exp(-100\rho_0((x - 0.3)^2 + (y - 0.3)^2)/p_0),$$

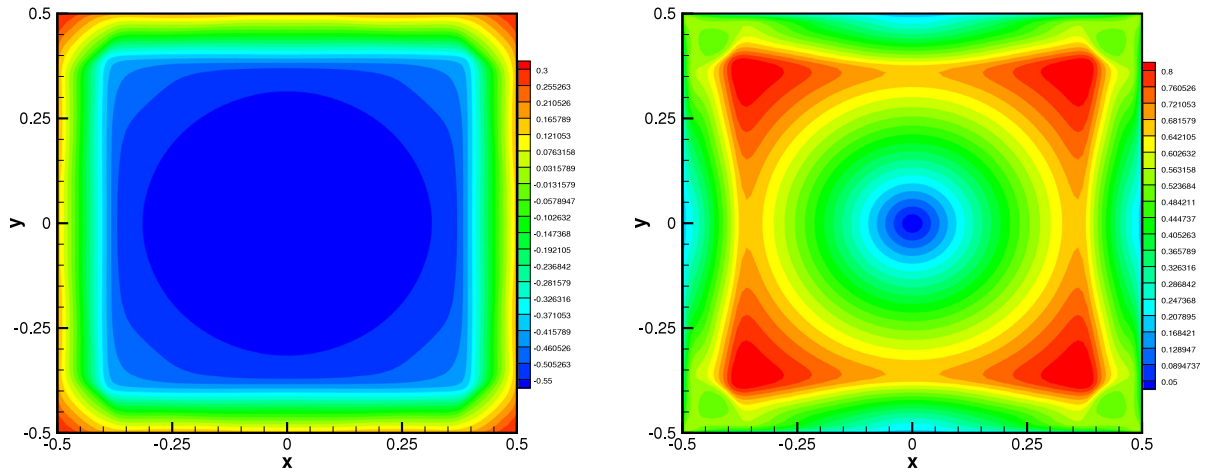


Fig. 5. The contours of the numerical results of the small amplitude wave propagation problem in Section 4.4.2 by non-well-balanced WENO schemes at time $t = 0.2$ with 100×100 points. Pressure perturbation (left) and velocity $(\sqrt{u^2 + v^2})$ (right).

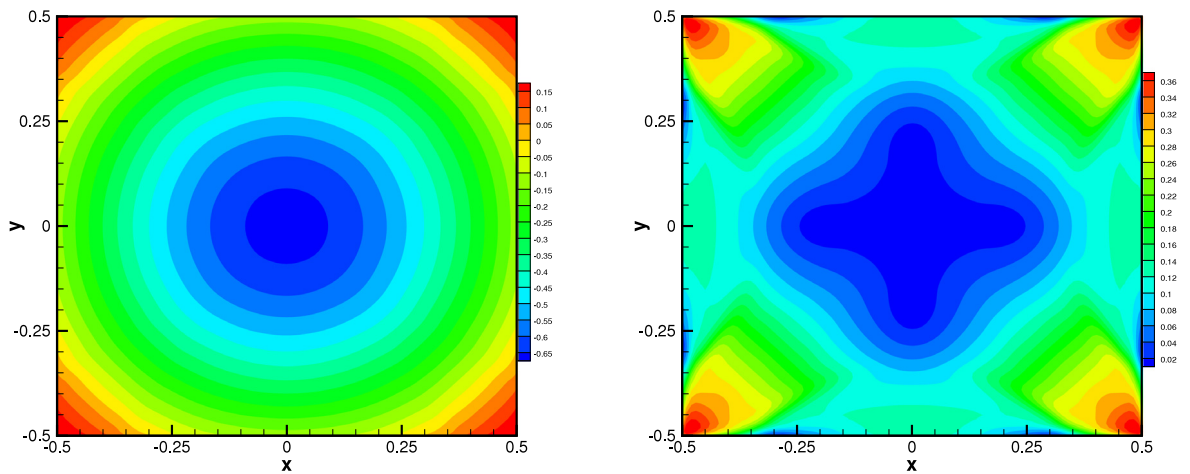


Fig. 6. The contours of the numerical results of the small amplitude wave propagation problem in Section 4.4.2 by well-balanced WENO schemes at time $t = 1.5$ with 100×100 points. Pressure perturbation (left) and velocity $(\sqrt{u^2 + v^2})$ (right).

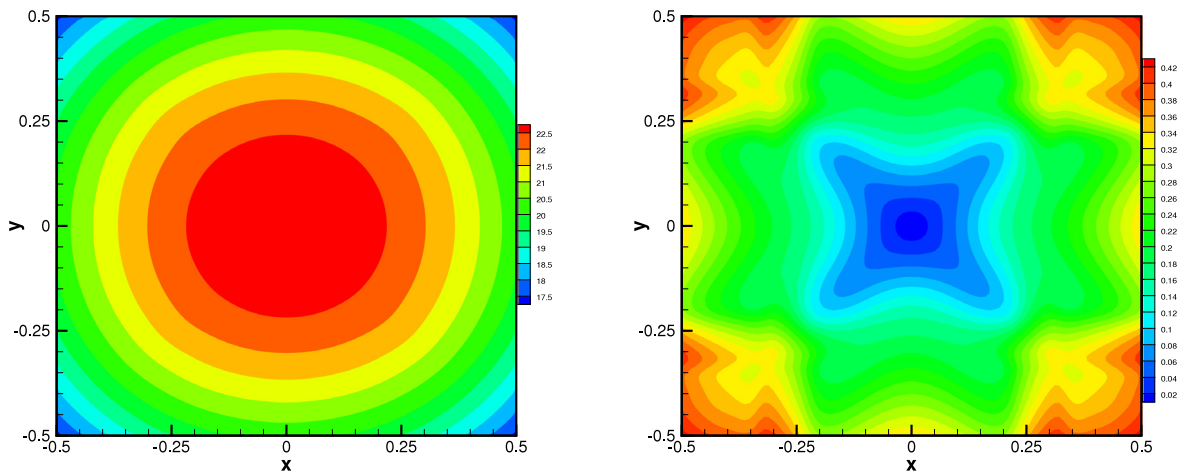


Fig. 7. The contours of the numerical results of the small amplitude wave propagation problem in Section 4.4.2 by non-well-balanced WENO schemes at time $t = 1.5$ with 100×100 points. Pressure perturbation (left) and velocity $(\sqrt{u^2 + v^2})$ (right).

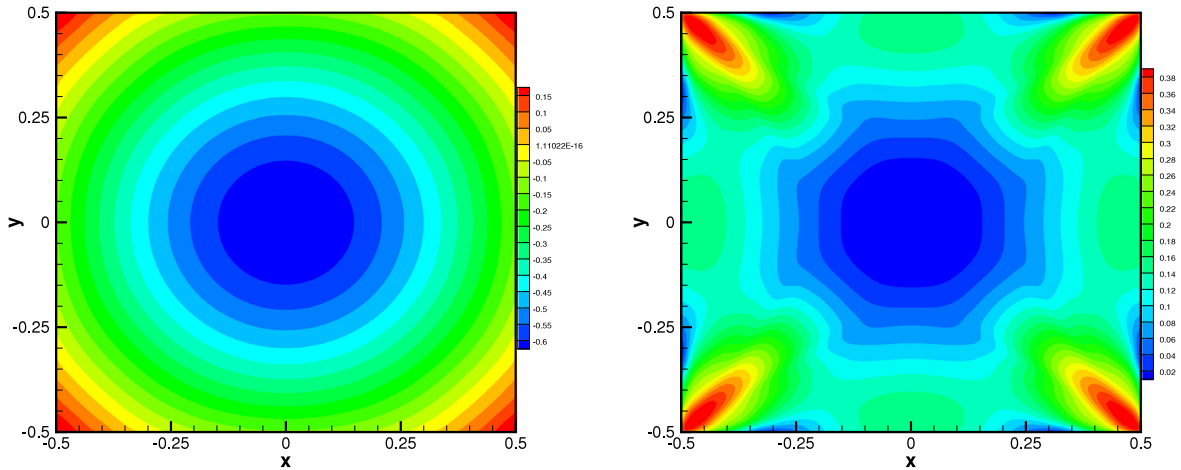


Fig. 8. The contours of the numerical results of the small amplitude wave propagation problem in Section 4.4.2 by well-balanced WENO schemes at time $t = 3$ with 100×100 points. Pressure perturbation (left) and velocity $(\sqrt{u^2 + v^2})$ (right).

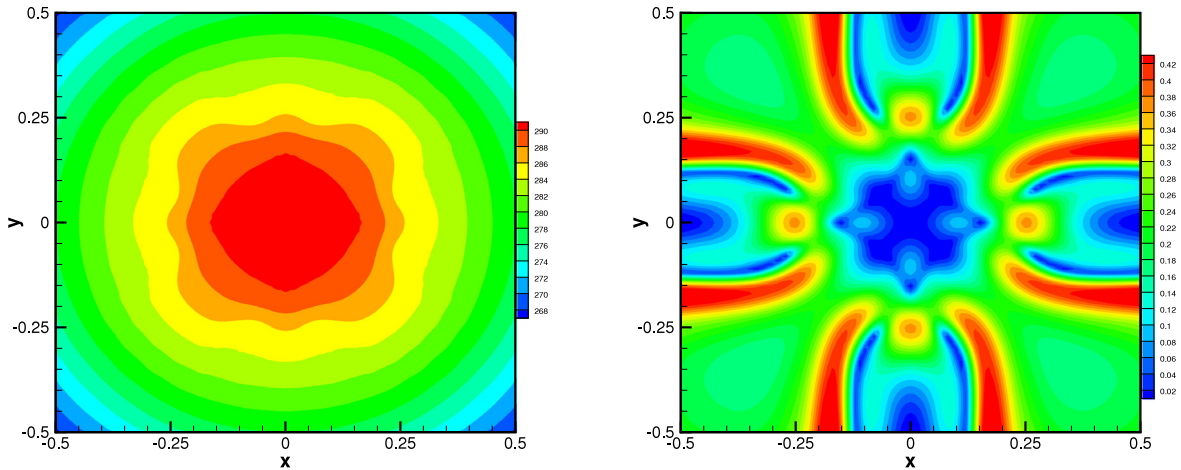


Fig. 9. The contours of the numerical results of the small amplitude wave propagation problem in Section 4.4.2 by non-well-balanced WENO schemes at time $t = 3$ with 100×100 points. Pressure perturbation (left) and velocity $(\sqrt{u^2 + v^2})$ (right).

with $\eta = 0.001$, $\rho_0 = 1.21$, $p_0 = 1$, and keep the velocity and density profiles to be the same. We present the numerical results at $t = 0.15$ by well-balanced WENO schemes in Fig. 10. For comparison, we also run the same test with non-well-balanced WENO schemes on the same mesh using the straightforward source term evaluation, and present the results in Fig. 11. Again, we can observe that non-well-balanced WENO schemes fail to capture such small perturbation on relatively coarse meshes, while the well-balanced ones can resolve it well with good resolution. Note that the magnitude of the pressure perturbation by non-well-balanced methods is much larger than that generated by well-balanced methods.

5. Concluding remarks

In this paper, we have constructed well-balanced finite difference WENO schemes for the one-dimensional and multi-dimensional Euler equations under static gravitational fields. Special attention has been paid to the approximation of the source term as well as the construction of the numerical fluxes, to achieve the well-balanced property. We have demonstrated that the proposed WENO schemes can balance the known equilibrium state exactly, and at the same time keep the high order accuracy for the general solutions. Extensive one- and two-dimensional tests are carried out to demonstrate these properties numerically.

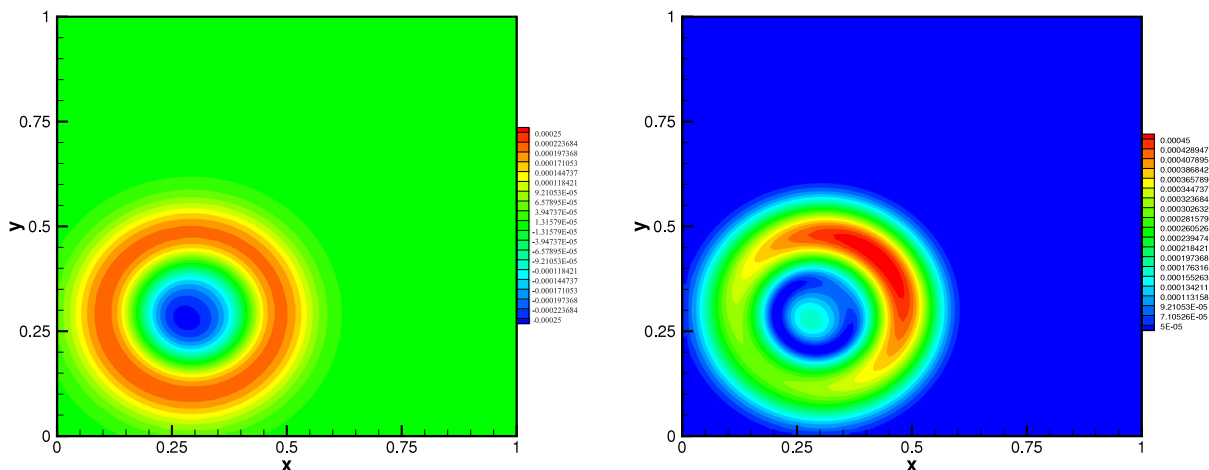


Fig. 10. Polytropic hydrostatic solution in Section 4.5 with $\eta = 0.001$ by well-balanced WENO schemes at time $t = 0.15$ on a mesh with 100×100 points. Pressure perturbation (left) and velocity ($\sqrt{u^2 + v^2}$) (right).

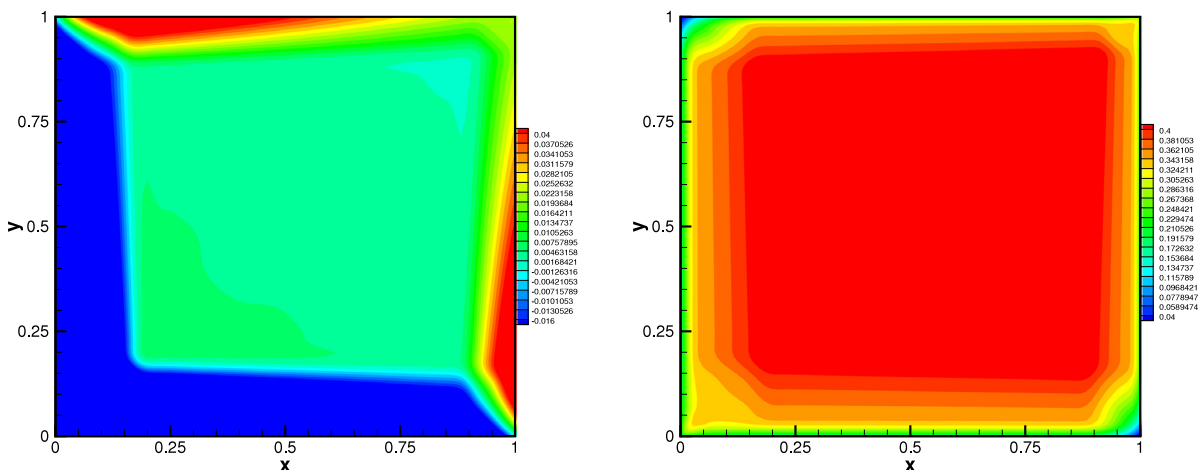


Fig. 11. Polytropic hydrostatic solution in Section 4.5 with $\eta = 0.001$ by non-well-balanced WENO schemes at time $t = 0.15$ on a mesh with 100×100 points. Pressure perturbation (left) and velocity ($\sqrt{u^2 + v^2}$) (right).

Acknowledgments

The research of the first author is supported by the National Natural Science Foundation of P.R. China (11201254, 11401332, 11771228) and the Project for Scientific Plan of Higher Education in Shandong Province of P.R. China (J12L108). This work was partially performed at the State Key Laboratory of Science/Engineering Computing of P.R. China by virtue of the computational resources of Professor Li Yuan’s group. The research of the second author is partially supported by NSF grants DMS-1621111, DMS-1753581 and ONR grant N00014-16-1-2714.

References

- [1] R.J. LeVeque, D.S. Bale, Wave propagation methods for conservation laws with source terms, in: Proceedings of the 7th International Conference on Hyperbolic Problems, 1998, pp. 609–618.
- [2] N. Botta, R. Klein, S. Langenberg, S. Lützenkirchen, Well-balanced finite volume methods for nearly hydrostatic flows, *J. Comput. Phys.* 196 (2004) 539–565.
- [3] C.T. Tian, K. Xu, K.L. Chan, L.C. Deng, A three-dimensional multidimensional gas-kinetic scheme for the navier-stokes equations under gravitational fields, *J. Comput. Phys.* 226 (2007) 2003–2027.
- [4] J. Luo, K. Xu, N. Liu, A well-balanced symplecticity-preserving gas-kinetic scheme for hydrodynamic equations under gravitational field, *SIAM J. Sci. Comput.* 33 (2011) 2356–2381.
- [5] R. Käppeli, S. Mishra, Well-balanced schemes for the euler equations with gravitation, *J. Comput. Phys.* 259 (2014) 199–219.

- [6] V. Desveaux, M. Zenk, C. Berthon, C. Klingenberg, A well-balanced scheme for the Euler equation with a gravitational potential, in: *Finite Volumes for Complex Applications VII-Methods and Theoretical Aspects*, in: Springer Proceedings in Mathematics & Statistics, vol. 77, 2014, pp. 217–226.
- [7] P. Chandrashekar, C. Klingenberg, A second order well-balanced finite volume scheme for Euler equations with gravity, *SIAM J. Sci. Comput.* 37 (2015) 382–402.
- [8] R. Käppeli, S. Mishra, A well-balanced finite volume scheme for the Euler equations with gravitation. The exact preservation of hydrostatic equilibrium with arbitrary entropy stratification, *Astron. Astrophys.* 587 (2016) A94.
- [9] Y. Xing, C.-W. Shu, High order well-balanced WENO scheme for the gas dynamics equations under gravitational fields, *J. Sci. Comput.* 54 (2013) 645–662.
- [10] G. Li, Y. Xing, Well-balanced discontinuous Galerkin methods for the Euler equations under gravitational fields, *J. Sci. Comput.* 67 (2016) 493–513.
- [11] G. Li, Y. Xing, High order finite volume WENO schemes for the Euler equations under gravitational fields, *J. Comput. Phys.* 316 (2016) 145–163.
- [12] G. Li, Y. Xing, Well-balanced discontinuous Galerkin methods with hydrostatic reconstruction for the Euler equations with gravitation, *J. Comput. Phys.* 352 (2018) 445–462.
- [13] D. Ghosh, E.M. Constantinescu, A well-balanced, conservative finite difference algorithm for atmospheric flows, *AIAA J.* 54 (2016) 1370–1385.
- [14] Y. Xing, C.-W. Shu, High order finite difference WENO schemes with the exact conservation property for the shallow water equations, *J. Comput. Phys.* 208 (2005) 206–227.
- [15] Y. Xing, C.-W. Shu, High-order well-balanced finite difference WENO schemes for a class of hyperbolic systems with source terms, *J. Sci. Comput.* 27 (2006) 477–494.
- [16] Y. Xing, C.-W. Shu, High order well-balanced finite volume WENO schemes and discontinuous Galerkin methods for a class of hyperbolic systems with source terms, *J. Comput. Phys.* 214 (2006) 567–598.
- [17] G. Jiang, C.-W. Shu, Efficient implementation of weighted ENO schemes, *J. Comput. Phys.* 126 (1996) 202–228.
- [18] C.-W. Shu, High order weighted essentially nonoscillatory schemes for convection dominated problems, *SIAM Rev.* 51 (2009) 82–126.
- [19] C.-W. Shu, Essentially non-oscillatory and weighted essentially non-oscillatory schemes for hyperbolic conservation laws, in: A. Quarteroni (Ed.), *Advanced Numerical Approximation of Nonlinear Hyperbolic Equations*, in: Lecture Notes in Mathematics, vol. 1697, Springer, 1998, pp. 325–432.